0273-2289/96/5758—0133$8.50

Kinetic and Modeling Investigation on Two-Stage Reverse-Flow Reactor as Applied to Dilute-Acid Pretreatment of Agricultural Residues

RONGFU CHEN,[1] YOON Y. LEE,*[,1] AND ROBERT TORGET[2]

[1]*Department of Chemical Engineering, Auburn University, AL 36849; and* [2]*National Renewable Energy Laboratory, Golden, CO*

ABSTRACT

The kinetics of dilute-acid pretreatment/hydrolysis of the hemicellulose in a mixture of corn cobs and corn stover was investigated. The kinetic data confirmed that the hemicellulose in this feedstock is of a biphasic nature. The kinetic model recognizes the presence of soluble xylose oligomers, xylose monomer, and the decomposition of xylose. The kinetic parameters were determined over the conditions of 120–150°C, and sulfuric acid concentration of 0.44–1.90%.

The biphasic nature of the kinetics brings about an additional flexibility in the reactor design and the operation strategy, since different reaction conditions can be applied to each of the two different fractions of hemicellulose in the feedstock. With incorporation of the kinetic data, a percolation reactor operated under various modes, uniform temperature, temperature step change (along with or without flow rate step change), and two-stage reverse-flow operation, was modeled and investigated for its performance. The modeling results affirmed that a step-change/reverse-flow operation is advantageous for biphasic substrates, including agricultural residues. The optimum temperature difference in the step-change operation was determined to be 30°C over a wide range of reaction temperature. Temperature step change alone (without use of reverse-flow mode) increased the product yield by 3–11% (depending on the reaction conditions) over that of uniform temperature operation. The most significant improvement, however, was seen with application of a two-stage reverse-flow reactor arrangement with temperature step change employing different conditions at each stage. This operation essentially doubled the sugar concentration over that of the temperature step change operation.

Index Entries: Dilute-acid pretreatment; kinetics, modeling; percolation; corn cobs/stover mixture.

Abbreviations: A, acid concentration; C_0, initial xylan concentration in percolation; E_i, activation energy for k_i; F1,F2, fast and slow fraction of hemicellulose; H, hemicellulose concentration; k_{oi}, frequency factor for k_i; k_i, rate constant = $A^{ni}k_{oi}\exp(E_i/RT)$, min^{-1}; L, reactor length, cm; n_i, acid concentration exponent; O, oligomer concentration; R, universal gas constant; S, dimensionless concentration;

*Author to whom all correspondence and reprint requests should be addressed.

t, time, min; T, absolute temperature, °K; u, velocity inside percolation reactor; x, distance coordinate along reactor length, cm; X, xylose concentration; Y, yield; z, x/L;

Greek: $\alpha_i, k_3/k_i, I = 1, 2; \beta_i, k_iL/u; \gamma_i, k_4/k_i, I = 1, 2; \rho, \tau_1/\tau; \tau, tu/L; \tau_1, \tau_2$, dimensionless time before and after temperature shifting in step-change mode; ω, ratio of velocity at high temperature to low temperature;

Subscript: 0, value at $t = 0$; 1, fast-hydrolyzing hemicellulose; 2, slow-hydrolyzing hemicellulose; O, oligomer; T, total; X, xylose.

INTRODUCTION

Dilute-acid hydrolysis of hemicellulose is one of the major process options applicable for biomass pretreatment. In this process, it is essential to consider the recovery of hemicellulose sugars as well as the effectiveness of the pretreatment. One common problem found in the acid pretreatment is that the sugars are decomposed under high temperature and low pH conditions to form undesirable components that are toxic to subsequent fermentation. Under the circumstances, it is critically important to choose proper reaction conditions, type of reactor, and mode of reactor operation. In our previous studies along these lines *(1–4)*, we have established that the percolation reactor (packed-bed flow through type) is one of the reactor types most appropriate for biomass pretreatment. In the application of this reactor, the sugar product is discharged from the reactor as it is formed. This permits the process to attain high sugar yield by minimizing the sugar decomposition.

The scope of our recent study on this subject was extended to cover agricultural residues including corn cobs/stover mixture (CCSM). Although some of the characteristics are similar among various biomass feedstocks, we found that the kinetic behavior of the hemicelluloses in various species differ significantly. We have reported that hemicellulose in hardwoods can be modeled as a biphasic substrate *(4,5)*, i.e., it is composed of two different fractions, fast-hydrolyzing and slow-hydrolyzing ones. We also found it to be true with CCSM. However, the reactions with CCSM are much more rapid than those of hardwoods, such that much less stringent conditions are required, i.e., lower temperature and/or acid levels. Under the lower temperature/acid conditions, the reaction pattern also changes so that soluble xylose oligomers appear as a recognizable component in the overall reaction of dilute-acid hydrolysis of the hemicellulose. These observations led us to modify our reaction model to account for the different kinetic pattern, including xylose oligomers as an additional component. This kinetic model is introduced here as an improved version over that of Kim et al. *(6)* in which the oligomer formation is neglected.

This investigation was undertaken first to establish a kinetic model that accounts for xylose oligomers as an additional entity and to determine the associated reaction kinetic parameters specifically applicable for acid hydrolysis of CCSM hemicellulose based on our experimental data of the kinetic study. The experimental conditions of interest were 120–150°C, and 0.44–1.90 wt% of sulfuric acid, substantially lower than those applied to hardwoods in both accounts. The mathematical modeling of a percolation reactor operated under various modes was then developed considering the kinetic pattern as well as the newly obtained kinetic parameters of CCMS. The modeling work covered operations under uniform temperature, two-stage step change, and two-stage step change reverse flow. The latter is a process scheme originally developed at the National Renewable Energy Laboratory (NREL) *(7)*.

EXPERIMENTAL METHODS

Materials

The CCSM feedstock was supplied in the form of milled fine particles (20–60 mesh) by NREL and used without any modification. The Cellulase Enzyme, Cytolase CL (Lot No 17-92262-09) was obtained from Environmental Biotechnologies, Inc. (Santa Rosa, CA).

Batch Reactions

For the kinetic study, reactions were carried out in Pyrex™ glass tube reactors (11-mm id). The reactors were packed with 0.4 g biomass and 6 mL acid solution, and sealed at both ends under natural gas–oxygen flame. To initiate the reaction, the glass reactor ampules were placed into an oil bath (Haake FS model) in which the temperature was preadjusted to a level 50°C higher than the desired point. After 50 s, the ampules were transferred into another oil bath preset at the desired reaction temperature. The two-oil-bath procedure was done to minimize the preheating time. Temperature measurement within a reactor has shown that the center section of the reactor reached the set point in 50 s. After being subjected to specified reaction times, the reactors were quenched in a cold water bath.

Analytical Methods

Sugar analyses for solid samples were performed according to the NREL CAT Standard Procedure No. 02 using high-performance liquid chromatography (HPLC) equipped with a refraction index (RI) detector, and Bio-Rad's (Hercules, CA) Aminex HPX-87P column. The liquid samples were analyzed for sugars by HPLC, RI detector, and Bio-Rad's Aminex HPX-87H column, with mobile phase of 0.005*M* sulfuric acid. The amount of soluble xylose oligomer in the hydrolysate (from primary hydrolysis) was measured by secondary hydrolysis with Cytolase CL enzyme. The increase in xylose after secondary hydrolysis was taken as xylose oligomers. All of the kinetic data analysis was done on the basis of xylose equivalent.

MODEL DEVELOPMENT

Kinetic Model

The sharp breakage in the semilog plot for the remaining xylan (Fig. 1) confirms that the xylan in CCSM is biphasic. This finding is in agreement with the kinetics of hemicellulose hydrolysis in other herbaceous biomass feedstocks, such as switchgrass *(8)*. With the recognition of xylose oligomer as a separate entity, the overall kinetic pattern of dilute-acid treatment of hemicellulose is now described as that shown in Fig. 2. For the proposed kinetic model, the variation of each individual component can be theoretically determined by the following set of differential equations:

$$(dH_1/dt) = -k_1H_1 \quad (1)$$

$$(dH_2/dt) = -k_2H_2 \quad (2)$$

$$(dO/dt) = k_1H_1 + k_2H_2 - k_3O \quad (3)$$

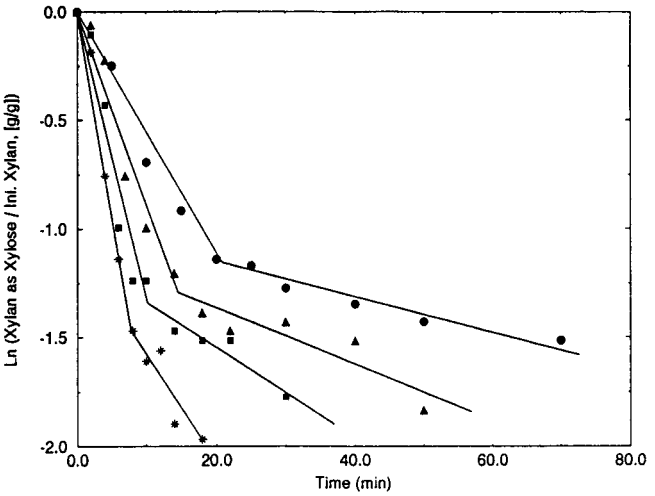

Fig. 1. Decay of xylan content in CCSM hemicellulose during hydrolysis (temperature = 140°C, solid:liquid = 1:16.4). ●, 0.47 wt% acid, ▲, 0.73 wt%, ■, 1.22 wt%, *, 1.95 wt%.

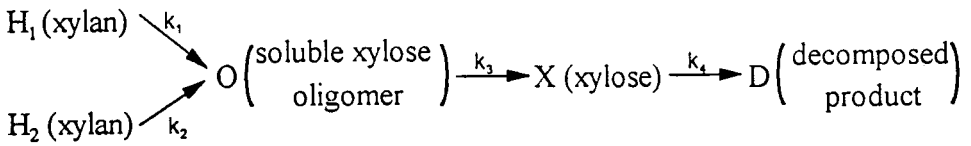

Fig. 2. Acid hydrolysis pathway of CCSM hemicellulose.

$$(dX/dt) = k_3O - k_4X \tag{4}$$

with initial conditions at $t = 0$, $H_1 = F_1 H_0$, $H_2 = F_2 H_0$, $O = 0$, $X = 0$.

The analytical solutions for eqs. *(1–4)* are obtained as follows:

$$O = \left(\frac{F_1H_0k_1}{k_3-k_1}\right)(e^{-k_1t}-e^{-k_3t}) + \left(\frac{F_2H_0k_2}{k_3-k_2}\right)(e^{-k_2t}-e^{-k_3t}) \tag{5}$$

$$X = \frac{F_1H_0k_1k_3}{(k_3-k_1)(k_4-k_1)}(e^{-k_1t}-e^{-k_4t}) + \frac{F_2H_0k_2k_3}{(k_3-k_2)(k_4-k_2)}(e^{-k_2t}-e^{-k_4t})$$

$$-\left(\frac{k_3}{k_4-k_3}\right)\left(\frac{F_1H_0k_1}{k_3-k_1}+\frac{F_2H_0k_2}{k_3-k_2}\right)(e^{-k_3t}-e^{-k_4t}) \tag{6}$$

Process Model of Percolation Reactor

The percolation reactor is a packed-bed, flow-through-type reactor, as shown in Fig. 3. In the following modeling procedure, it is assumed that the axial heat transfer after temperature step change and the internal and external diffusion effects are negligible.

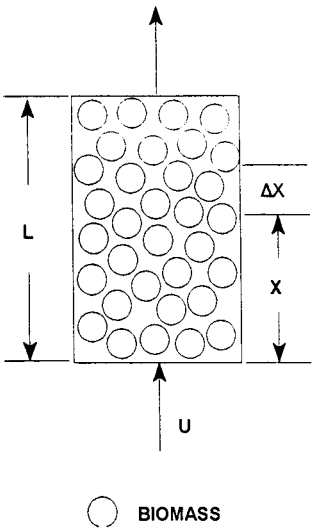

Fig. 3. Conceptual sketch of percolation reactor.

Uniform Temperature Operation

Material balance on component O (oligomers) leads to the following:

$$(\partial O/\partial \tau) = (k_1H_1 + k_2H_2 - k_3O) - u[(\partial O/\partial x)] \tag{7}$$

where

$$H_1 = F_1H_0\exp\{-k_1[t-(x/u)]\},\ t > (x/u)$$
$$H_2 = F_1H_0\exp\{-k_2[t-(x/u)]\},\ t > (x/u) \tag{8}$$

The pertinent initial and boundary conditions are: $x = 0$, $O = 0$, and $t = 0$, $O = 0$. The equation regarding fast hemicellulose is:

$$(\partial O_1/\partial \tau) = (k_1H_1 + k_3O_1) - u(\partial O_1/\partial x) \tag{9}$$

where H_1 is shown in Eq. (8). In dimensionless form, the PDE is expressed as:

$$(\partial S_{O1}/\partial \tau) = \beta_1\exp[-\beta_1(\tau - z)] - \alpha_1\beta_1S_{O1} - (S_{O1}/\partial z) \tag{10}$$

with pertinent initial and boundary conditions of $t = 0$, $S_{O1} = 0$, and $z = 0$, $S_{O1} = 0$.

By the Laplace Transform method, one obtains the following solution for Eq. (10):

$$S_{O1} = (1/\alpha_1)(1 - \exp-\alpha_1\beta_1z)\exp-\beta_1(\tau - z) \tag{11}$$

The yield of oligomer from fast hemicellulose is then calculated by integrating S_{X1} value at the reactor exit point ($z = 1$) over the range of operation time $1 \sim 1 + \tau$:

$$Y_{O1} = \int_1^{\tau+1} (S_{O1})_{z=1}d\tau = [1 - \exp(-\alpha_1\beta_1)]/(\alpha_1\beta_1)\ [1 - \exp(-\beta_1\tau)] \tag{12}$$

Oligomer yield from slow hemicellulose Y_{O2} is identical to that shown in Eq. (12) with subscript value of 2 replaced by 1. The combined yield of soluble xylose oligomer from both fast and slow hemicellulose can be expressed as:

$$Y_O = F_1Y_{O1} + F_2Y_{O2} \tag{13}$$

Similarly, material balance for xylose from fast hemicellulose leads to the following:

$$(\partial S_{X1}/\partial \tau) = \alpha_1\beta_1 S_{O1} - \gamma_1\beta_1 S_{X1} - (\partial S_{X1}/\partial z) \tag{14}$$

where S_{O1} is given by Eq. (11).

The solution for Eq. (14), xylose from fast hemicellulose, is expressed as:

$$S_{X1} = \frac{1}{\gamma_1} e^{\beta_1 z}\left(e^{-\beta_1 \tau} - e^{-\beta_1(1+\gamma_1)\tau}\right) +$$

$$\frac{1}{\gamma_1} e^{-\gamma_1\beta_1 z}\left(e^{-\beta_1(1+\gamma_1)(\tau - z)} - e^{-\beta_1(\tau - z)}\right) +$$

$$\frac{e^{-\beta_1 \tau}}{\gamma_1 - \alpha_1}\left(e^{\beta_1(1-\gamma_1)z} - e^{\beta_1(1-\alpha_1)z}\right) \tag{15}$$

The yield of xylose from fast hemicellulose is obtained as:

$$Y_{X1} = \int_1^{\tau+1} (S_{X1})_{z=1} = \frac{1}{\gamma_1} e^{\beta_1}\left(\frac{e^{-\beta_1} - e^{-\beta_1(\tau+1)}}{\beta_1} + \frac{e^{-\beta_1(1+\gamma_1)(\tau+1)} - e^{-\beta_1(1+\gamma_1)}}{\beta_1(1+\gamma_1)}\right) +$$

$$\frac{1}{\gamma_1} e^{-\gamma_1\beta_1}\left(\frac{1 - e^{-\beta_1(1+\gamma_1)\tau}}{\beta_1(1+\gamma_1)} + \frac{e^{-\beta_1\tau} - 1}{\beta_1}\right) +$$

$$\frac{e^{\beta_1(1-\gamma_1)} - e^{\beta_1(1-\alpha_1)}}{\gamma_1 - \alpha_1}\left(\frac{e^{-\beta_1} - e^{-\beta_1(\tau+1)}}{\beta_1}\right) \tag{16}$$

The yield of xylose from slow hemicellulose Y_{X2} is identical to Eq. (16) with subscript value of 2 replaced by 1. The total yield of sugar including soluble xylose oligomer and xylose monomer, is expressed as:

$$Y_T \text{ (uniform)} = F_1(Y_{O1} + Y_{X1}) + F_2(Y_{O2+} Y_{X2}) \tag{17}$$

Two-Stage Step-Change Operation

The term τ_1 represents the dimensionless reaction time up to the temperature shifting point, and τ_2 represents the rest of the reaction time. Total yield consists of four parts, namely, fast fraction reacting for the duration of τ_1, slow for τ_1, fast for τ_2, and slow for τ_2. The total yield is then expressed as:

$$Y_T(\text{step}) = F_1[Y_{O1,T1} + Y_{X1,T1} + R_1(Y_{O1,T2} + Y_{X1,T2})] +$$
$$F_2[Y_{O2,T1} + Y_{X2,T1} + R_1(Y_{O2,T2} + Y_{X2,T2})] \tag{18}$$

where:

$$R_1 = \exp(-\beta_1\tau_1)$$
$$R_2 = \exp(-\beta_2\tau_1) \tag{19}$$

The yield is now expressed as a function of reaction time and a number of dimensionless parameters including $\beta_1 (=k_1 L/u)$. In actual computation of yields, τ

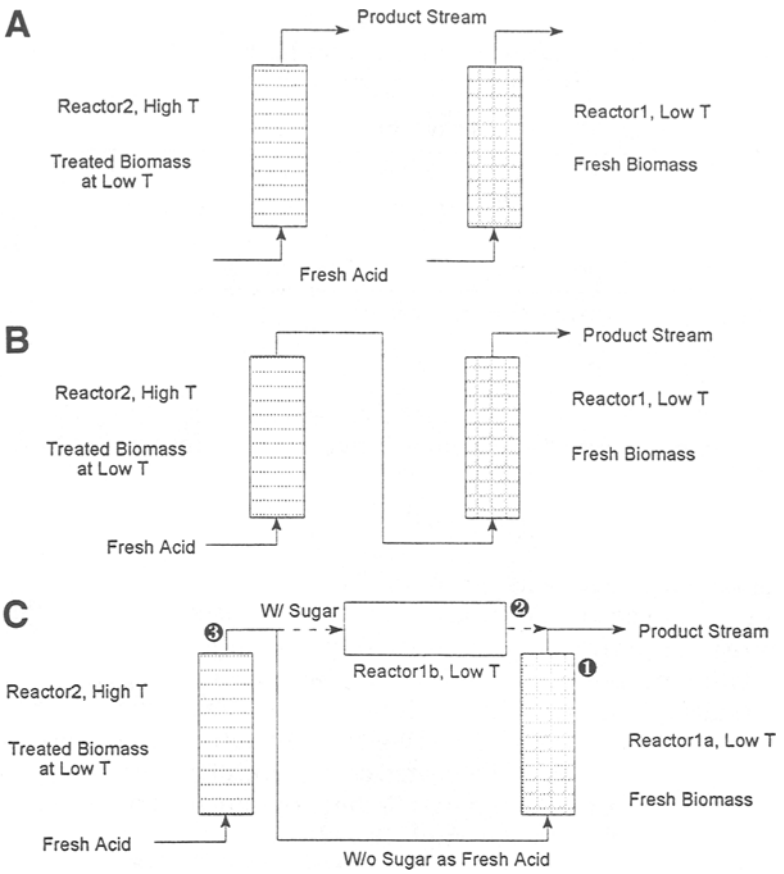

Fig. 4. Schematics of temperature step change and two stage reverse flow in modeling study. **(A)** Two-stage step change, **(B)** two-stage reverse flow, **(C)** two-stage reverse flow (artificial).

value is first set, and then the optimum β_1 is computed (to maximize the yield value) using Eq. (20) before the integration process.

$$\left(\frac{\partial Y_T}{\partial \beta_1}\right)_{\alpha,\tau} = \left(\frac{\partial Y_T}{\partial \beta_1}\right)_{\alpha,\tau,\beta_2} + \left(\frac{\partial Y_T}{\partial \beta_2}\right)_{\alpha,\tau,\beta_1}\left(\frac{\partial \beta_2}{\partial \beta_1}\right)_{\alpha,\tau} = 0 \tag{20}$$

where $\beta_2 = (k_2/k_1)\,\beta_1$.

Two-Stage Reverse-Flow Operation

As depicted in Fig. 4C, a two-stage reverse-flow operation can be simulated as a two-stage step-change operation with a bypass reactor (Reactor 1b). The results from Reactor 1a are the same as those from the first stage reactor in two-stage step-change operation, Reactor 1 in Fig. 4A. The results from Reactor 2 are the same as those from the second-stage reactor in two-stage step-change operation, Reactor 2 in Fig. 4A. The yields from Reactor 1b can be calculated by the following equations:

Xylose yield = xylose from Reactor 2 + xylose generated from oligomer in Reactor 1b - xylose decomposed in Reactor 1b (21)

Table 1
Activation Energy for Each Reaction

k_i	k_{0i} min^{-1} (%w/w)$^{-ni}$	n_i	E_i, kcal/g mol
1	1.998×10^{10}	1.0	20.6
2	1.237×10^{13}	1.0	27.7
3	1.046×10^{14}	1.2	27.5
4[a]	8.990×10^{11}	1.0	28.2

[a]After Kim and Lee *(5)*.

Oligomer yield = oligomer
from Reactor 2 – oligomer converted to xylose in Reactor 1b (22)

RESULTS AND DISCUSSION

The kinetic model was set to follow the pattern of parallel-serial reactions shown in Fig. 2. The kinetic information was then used in the simulation of a percolation reactor performing dilute-acid pretreatment/hemicellulose hydrolysis. For simulation purposes, a computer program was developed on the basis of theoretical results described in the previous section. The program incorporates experimentally determined kinetic data as well as the solution of modeling equations. The optimization process involved repeated calculation of yields changing the operation parameters. In the optimization part of the program, the Fortran subroutines from IMSL, Inc. (Houston, TX) were employed *(9)*.

Determination of Kinetic Parameters

Equations (8) and (9) were used to determine the kinetic parameters. For this purpose, the experimental data taken at 120, 130, 140, and 150°C were put through a nonlinear regression using the SAS NLIN Program *(10)*. The xylose decomposition data (k_4) were taken from Kim and Lee *(5)*. The regression for parameter estimation was done in two tiers. For a given set of four parameters of F_f (the fast hydrolyzable fragment) n_1, n_2, and n_3, the remaining 12 parameters (four each for k_1, k_2, and k_3 at four different temperature levels) were determined by nonlinear regression analysis. This process was repeated varying the four aforementioned parameters until the minimum of the sum of square of errors was attained. The best fitting values of F_f, n_1, n_2, and n_3 were found to be 0.65,1.0, 1.0, and 1.2 respectively. The rest of the kinetic parameters are shown in Table 1.

The comparison between predicted reaction progress based on the kinetic model and the actual experimental data is shown in Fig. 5. The model prediction is seen to be in good agreement with the experimental data. Hence, it is confirmed that the proposed kinetic model and the associated kinetic parameters are valid.

Optimum Temperature Step Change

Kim et al. *(4)* reported that the performance in a percolation reactor can be improved by adopting a step change in operating conditions over that of uniform operating condition. The step-change temperature strategy was further refined to

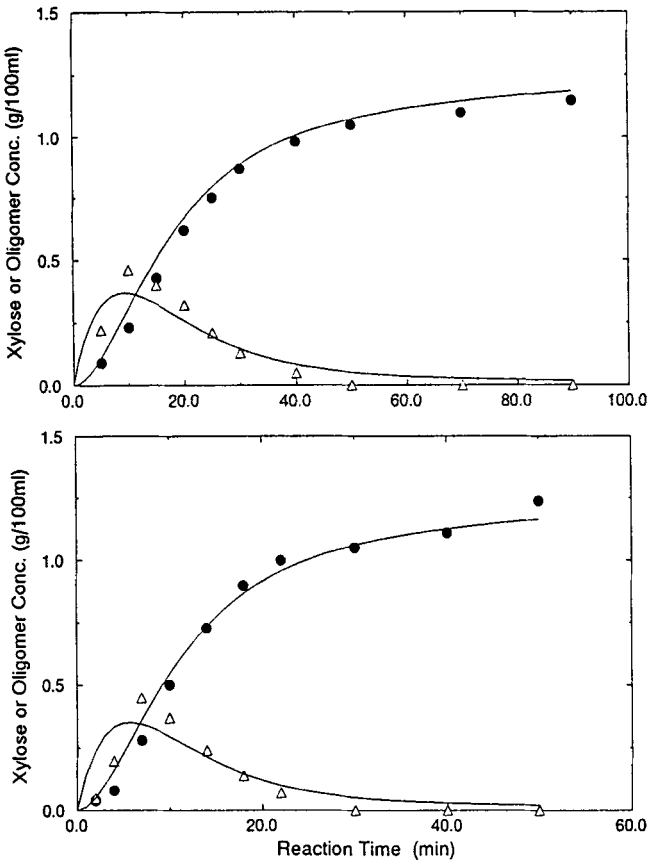

Fig. 5. Comparison between the predicted and experimental value on reaction progression in CCSM hydrolysis at 140°C, acid conc.=0.44 and 0.68% (point = experimental values, line = calculated kinetic model values). **(A)** Acid concentration, 0.44%, solid:liquid, 1:16.4. **(B)** Acid concentration, 0.68%, solid:liquid, 1:16.4. –, model predicted value; ●, xylose (experimental data); △, oligomer (experimental data).

obtain an optimum level of temperature difference. Temperature differences of 10, 20, 30, and 40°C were applied in the study with low temperatures set at 120, 130, and 140°C. The highest yield occurred with temperature differences of 30°C for low temperatures of 130 and 140°C, and 40°C for a low temperature of 120°C (Fig. 6). The temperature difference of 30°C was then taken as the optimum, ignoring the results at 120°C, a temperature unacceptable for this substrate because of low reaction rate and yield. The step-change operation brought about 8.8–10.9% improvement in yield over that of uniform low-temperature operation, and 2.9–3.5% over uniform high-temperature operation.

Optimum Flow Rate Step Change (Along with Temperature Step Change)

The preceding simulation of temperature step change was conducted with a constraint that the liquid flow rate was kept constant for the entire operation. Since β is an operational parameter related not only to temperature, but also the flow rate,

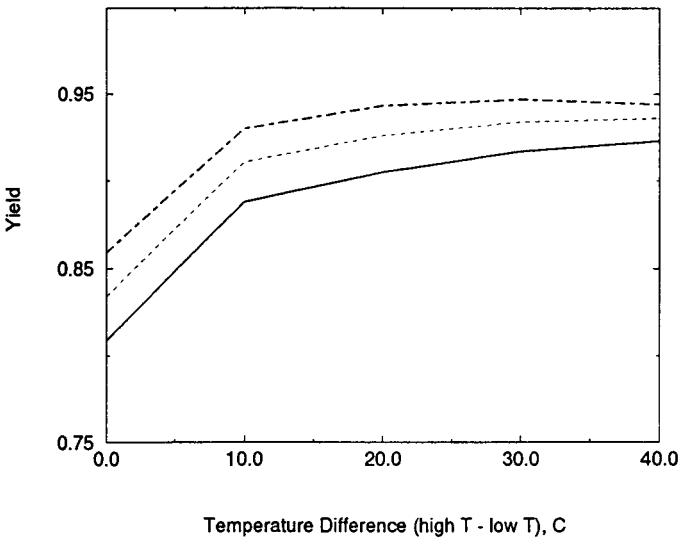

Fig. 6. Modeling results on effect of temperature difference on yield in step-change operation (acid conc. = 0.8%, τ = 1.5, ρ = 0.5). (---) low T = 140°C; (—) low T = 130°C; (-) low T = 120°C.

it is probable that the β value shift (change of liquid velocity and/or temperature) may also influence the sugar yield. To verify this, the velocity ratio ω was introduced as an additional adjustable parameter in the percolation reactor simulation program. The velocity ratio ω was defined as the velocity in high-temperature operation to the velocity in the low-temperature operation. Figure 7 shows the effect of ω on product yield. It is seen that the maximum yield occurs at ω = 2.0 for all three cases. The additional improvement of yield owing to ω adjustment was 0.4–0.6%.

Two-Stage Reverse-Flow Operation

Two-stage reverse-flow percolation reactor design was proven to be advantageous in obtaining high product concentration theoretically *(6)* and experimentally *(11)*. The concept of the process is shown in Fig. 4B. The biomass is first treated at a low temperature in percolation mode. It is then treated again at a high temperature. Up to this point, the procedure is identical to the two-stage process with a step change in temperature. The difference is that the stream from the high-temperature treatment is again put through a reactor packed with fresh biomass at low temperature. The reacted solid residue in this reactor is then treated with fresh acid at high temperature. This process is repeated. The difference between two-stage step-change and two-stage reverse-flow configurations is depicted in Fig. 4. For computation purpose, it is postulated that Reactor 1 in Fig. 4B is composed of two artificial reactors (superposition), namely Reactor 1a containing fresh biomass with input stream as fresh acid without sugar content and Reactor 1b containing no biomass with sugar stream input. The process composed of Reactor 1a and Reactor 2 (Fig. 4C) is in fact identical to the two-stage step-change operation shown in Fig. 4A.

There are two important points in the role of the two-stage reverse-flow reactor. One is the advantage of superposition, which can combine two sugar streams together (from Reactor 1a and Reactor 1b), thus increasing the product concentra-

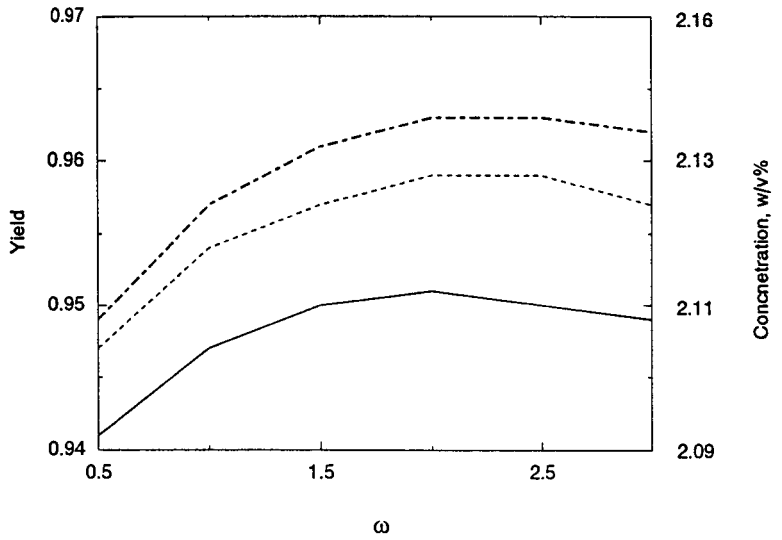

Fig. 7. Modeling results on effect of flow rate ratio on product yield (acid conc. = 0.8%, τ = 1.5, ρ = 0.5). (--) 140–170°C; (—) 130–160°C; (–), 120–150°C.

tion. Another is the disadvantage of decomposing the sugar products inside Reactor 1b. The key issue in the two-stage reverse-flow mode is that because of the low temperature applied in Reactor 1b (Reactor 1), the sugar decomposition inside Reactor 1b is in fact minimized. There are three different flow arrangements that are available for the two-stage step-change process as indicated in Fig. 8. Depending on the acid throughput applied at each stage of the process, the process stream for low-temperature processing is either supplemented with fresh acid or partially bypassed to the sugar product. In Fig. 8B, make-up fresh acid is introduced to the system. The product concentration is therefore expected to decrease. Furthermore, the bypass stream in Fig. 8C not being subjected to superposition, the product concentration is also expected to be lower than that of Fig. 8A. Thus, Fig. 8A would generally be regarded as a preferred mode of operation.

There is an important aspect of the percolation reactor that needs to be brought up in assessing its performance. In percolation reactor operation, the yield generally increases with τ, whereas the product concentration decreases with it. An inverse relationship, or a trade-off from a practical viewpoint, thus exists between the yield and the product concentration. The yield value alone without the corresponding concentration will not serve as a meaningful performance indicator.

The results of the simulation with optimized process parameters are summarized in Fig. 9. The yield values are indeed shown to follow the inverse relationship with product concentration. When the yield is compared at a fixed product concentration level, the two-stage reverse-flow mode gives highest yield, 96.5% at τ = 2 and 98% at τ = 3, followed by step change, uni-high, and uni-low. The advantage of reverse flow in attaining high product concentration is phenomenal, almost doubling the product concentration of step-change mode. The advantage of the superposition (the product stream coming out of one reactor being put through a second reactor) is clearly demonstrated here. The concentrations from the other three modes are in the order of step change > uni-high > uni-low. It is also noteworthy that

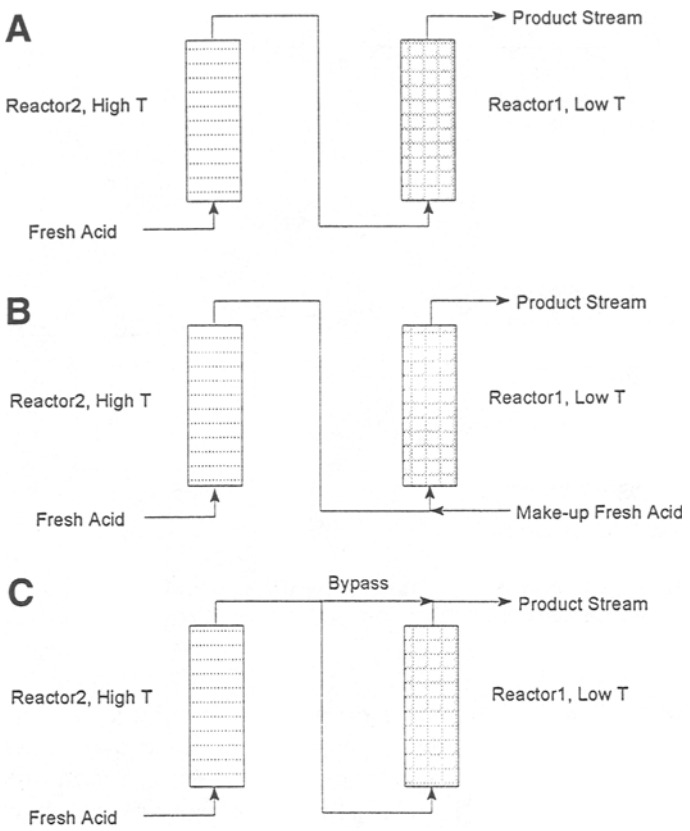

Fig. 8. Flow configuration in two-stage reverse-flow percolation reactor. **(A)** In(reactor 1) = out(reactor 2), $\rho = 0.5$); **(B)** in(reactor 1) = out(reactor 2) + fresh acid, $0.5 < \rho < 1.0$, **(C)** in(reactor 1) = out(reactor 2) - bypass, $0 < \rho < 0.5$.

for a given τ value (fixed amount of liquid throughput), step-change gives the highest yield, reverse flow the second highest, and uni-low the lowest yield. For the step-change mode, an optimum ρ was taken for a specific τ value. This is done so as to compare the optimum step-change mode with reverse flow. Although the reverse-flow mode gives highest product concentration, it also pays a price for it: additional sugar decomposition in Reactor 1. Sugar decomposition in Reactor 1 depends on the input sugar concentration. Yield loss in reverse flow can be as high as 2.8% at $\tau = 1.0$ with product concentration of 6.02 %(w/v), but as low as 0.2% at $\tau = 3.0$ with product concentration of 2.18%(w/v). Here again is a clear case of the trade-off between the product concentration and product yield. The true optimum operating condition can only be determined from consideration of overall process economics, which must include the cost of down stream processing.

Sugar Distribution in Reverse-Flow Mode

It is important to delineate the functions of the two separate reactors employed in the two-stage reverse-flow operation mode. Table 2 lists the sugar concentration at various points of the process (*see* Fig. 4C) from each fraction. Under the listed process condition, it is seen that 86.2% of fast-hydrolyzing hemicellulose, and only 19.4% of slow-hydrolyzing hemicellulose were recovered from a low-temperature

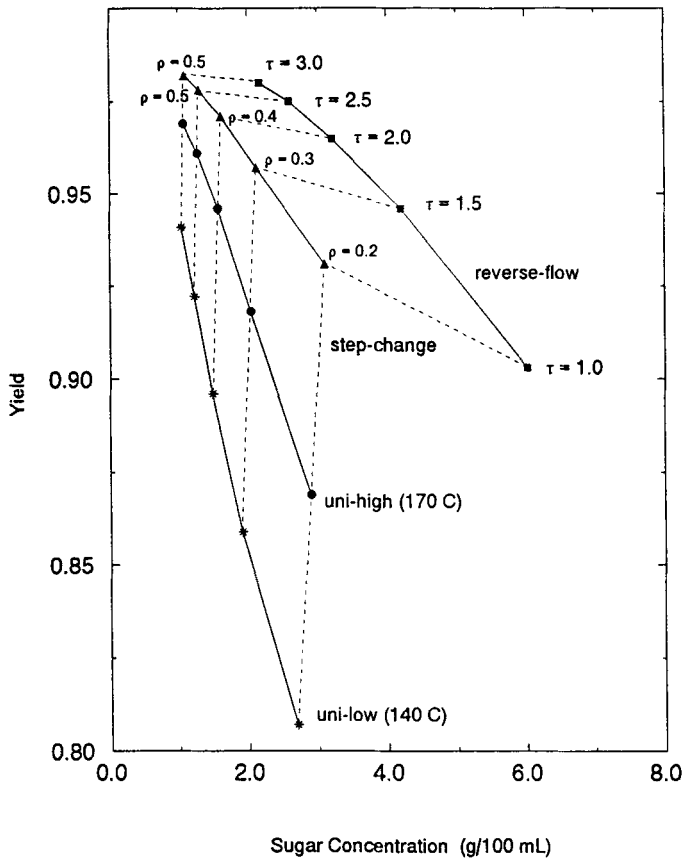

Fig. 9. Modeling results on yield vs sugar product concentration under various operation modes of percolation reactor (acid conc. = 0.8%, C_0 = 3.333 w/v%) (ρ: optimum values for step change, 0.5 for reverse flow).

reactor (Reactor 1a), whereas 67.4% of slow-hydrolyzing hemicellulose and only 12.9% of fast-hydrolyzing hemicellulose were recovered from a high-temperature reactor (Reactor 2). These results prove that the main reason for the existence of variational optimal temperature is the biphasic nature of the hemicellulose in the CCSM. The sugar stream passing through the Reactor 1b has decreased from 0.084 + 0.236 = 0.320 to 0.0006 + 0.315 = 0.3156 owing to decomposition, a mere 1.4% sugar loss. As we expected, oligomer formation was high in the low-temperature reactor (Reactor 1) and low in the high-temperature reactor (Reactor 2). This observation also agreed well with the results of the kinetic study.

CONCLUSIONS

The hemicellulose in CCSM is biphasic when it is subjected to dilute-acid hydrolysis. The biphasic kinetic model, including xylose oligomer and monomer, has shown good agreement with experimental data. On the basis of this kinetic data, a mathematical model was established, and process simulations were conducted for a percolation reactor operated under various modes. The optimum temperature difference in temperature step-change operation was found to be 30°C. The product

Table 2
Modeling Results of Product Sugar Distribution from Two-Stage Reverse-Flow Operation (low T = 140°C, high T = 170°C, τ = 1.5, and ρ = 0.5)

Location	Sugar source	Oligomer yield	Xylose yield	Total yield	Sugar recovered[a]
Reactor 1a	Fast fraction	0.179	0.381	0.560	0.862
	Slow fraction	0.022	0.046	0.068	0.194
Reactor 1b	Oligomer	0.0006	—	0.0006	—
	Xylose	—	0.315	0.315	—
Reacto 2	Fast fraction	0.003	0.081	0.084	0.129
	Slow fraction	0.009	0.227	0.236	0.674

[a]Sugar recovered = sugar received/sugar available from each fraction = total yield/F_i, where i = 1, 2.

yield in temperature step-change operation was substantially higher than that of uniform temperature operation at either limit. The application of flow rate step-change along with temperature step change brought about additional improvement of yield over the case with temperature step change alone. Use of a two-stage reverse-flow percolation reactor arrangement has brought about a significant improvement in the performance in that it has doubled the product concentration over that of two-stage step-change operation.

ACKNOWLEDGMENT

This research was supported by NREL through a Subcontract-XAW-3-13441-01.

REFERENCES

1. Lee, Y. Y., Lin, C. M., Johnson, T., and Chambers, R. P. (1978), *Biotechnol. Bioeng. Symp.* **8,** 75–88.
2. Limbaugh, M. L. (1980), MS Thesis, Auburn University, AL.
3. Cahela, D. R., Lee, Y. Y., and Chambers, R. P. (1983), *Biotechnol. Bioeng.* **25,** 3–17.
4. Kim, B. J., Lee, Y. Y., and Torget, R. (1993), *Appl. Biochem. Biotechnol.* **39,** 119–129.
5. Kim, S. B. and Lee, Y. Y. (1987), *Biotechnol. Bioeng. Symp.* **17,** 71–84.
6. Kim, B. J., Lee, Y. Y., and Torget, R. (1994), *Appl. Biochem. Biotechnol.* **45,** 113–129.
7. Torget, R. W., Hsu, T.-A., Kadam, K., and Phillippidis, G. P., and Wyman, C. E. (1993), Prehydrolysis of Lignocellulosic Materials, US Patent applied for.
8. Lee, Y. Y., Kim, B. J., and Chen, R. (1993), Final Report for Subcontract-NREL-XD-1-11121-1.
9. FORTRAN Subroutines for Mathematical Applications, User's Manual, IMSL, Inc., Houston, TX, (1991), p. 1096–1102.
10. Freund, R. and Littell, R. (1992), *SAS System for Regression,* 2nd ed., SAS Institute Inc., Cary, NC, p. 169–188.
11. Torget, R. W., Hayward, T. K., Hatzis, C., and Philippidis, G. P. (1995), presented at the 17th Symposium on Biotechnology for Fuels and Chemicals, Vail, CO.